

X-Ray Spectroscopic Study of the Electronic Structure of Visible-light Responsive N-, C- and S-Doped TiO₂

Xiaobo Chen¹, Per-Anders Glans^{2,3}, Xiaofeng Qiu¹, Smita Dayal¹, Wayne D Jennings⁴,
Kevin E. Smith², Clemens Burda¹, Jinghua Guo^{3*}

¹*Center for Chemical Dynamics & Nanomaterials Research, Department of Chemistry,
Case Western Reserve University, Cleveland, OH 44106, USA*

²*Department of Physics, Boston University, Boston, MA 02215, USA*

³*Advanced Light Source, Lawrence Berkeley National Laboratory, Berkeley, CA 94720,
USA*

⁴*Department of Materials Science and Engineering, Case Western Reserve University,
Cleveland, OH 44106, USA*

Abstract

The electronic origin of the visible-light response of N-, C- and S-doped TiO₂ has been studied using x-ray absorption, x-ray emission, and x-ray photoelectron spectroscopies. New electronic states are observed in the bulk band gap, above the valence band edge of pure TiO₂, which can be directly related to the visible-light absorption of the N-, C- and S-doped TiO₂ materials.

Key words: Electronic structure, Doped TiO₂, X-ray absorption, X-ray emission,
X-ray photoelectron

1. Introduction

Titanium dioxide (TiO_2) has been the subject of extensive studies since the late 1960s, due to its various applications in pigments, photoconductors, dielectric materials, and photocatalysts.¹⁻⁹ The wider application of TiO_2 as a photocatalyst can be realized by expanding its UV or near-UV absorption properties into visible-light region.⁶⁻¹⁴ Doping TiO_2 with different elements such as nitrogen (N), carbon (C), and sulfur (S) has shown promising results for visible-light photocatalysis.⁶⁻¹⁴ Titanium nitride (TiN) and carbide (TiC) are both metallic conductors with a partially filled band at the Fermi level (E_F) and a chemical bond of simultaneously metallic, covalent, and ionic character,¹⁵⁻²¹ while titanium sulfide (TiS_2) is regarded as a semiconductor or semimetal,^{22,23} with a bandgap of about 0.9 eV.²⁴ It is known that TiN, TiC, and TiS_2 can be oxidized to become TiO_2 via high-temperature sintering in air or oxygen.¹⁶⁻¹⁸ It has also been reported that C- and S-doped TiO_2 can be formed by heating TiC^{14,25} and TiS_2 powders^{13,26} at high temperatures. The oxidation of these materials provides an attractive technique to prepare doped TiO_2 with visible-light absorption.

The electronic structure of TiO_2 is well understood both theoretically and experimentally,²⁷⁻³⁸ and is characterized by a band gap located between the oxygen $2p$ valence band and the titanium $3d$ conduction band.²⁷ X-ray absorption spectroscopy (XAS) and X-ray emission spectroscopy (XES) are powerful element-specific probes of the electronic structure of materials, and have been applied extensively to study pure TiO_2 .^{16-21,24,27-39} In XAS, a core-level electron absorbs an x-ray photon and is excited to an unoccupied state above E_F .^{15,17,27,38} In XES, a valence band electron relaxes to a core hole created by the x-ray absorption process via the emission of an x-ray photon.^{19,29,32,36}

In x-ray photoelectron spectroscopy, a core-level electron is excited above the vacuum level by the incident light and the kinetic energy of the emitted electrons is recorded. XAS and XES spectra reflect the element specific conduction and valence band partial density of states (PDOS), respectively.^{40,41} In contrast, XPS measures the total density of states (DOS) of the valence band, as well as the kinetic energy of the core-level electrons (thus, the binding energy of the core-level electrons can be derived.).^{20,38,42-46} Thus, by combining XAS, XES and XPS results, a comprehensive understanding of the electronic structure of these materials can be achieved

We report here an XES, XAS, and XPS study of the electronic structure of N-, C- and S-doped TiO₂, as well as that of pure TiO₂. We have observed occupied states in the bulk band gap for the doped materials. These states do not exist in pure TiO₂, and likely related to the visible light properties of the doped oxides.

2. Experimental

The TiN, TiC and TiS₂ were purchased from Strem Chemicals as powders. The N, C and S-doped TiO₂ samples were prepared by oxidation of the above reagents at 1000°C for 6 hours in a quartz tube under atmosphere inside a Lindberg tube furnace with a digital temperature control unit. These samples were then allowed to cool, and doped TiO₂ was obtained. Pure TiO₂ was obtained by heating at 1000°C for 6 hours in air a TiO₂ powder prepared via a commonly used sol-gel method.⁴⁷

X-ray diffraction (XRD) patterns were obtained using a Philips PW 3710 X-ray powder diffractometer. The UV-visible reflectance spectra were measured on a Cary 50 UV-visible spectrometer with a reflectance unit.

The X-ray spectroscopic experiments were measured at the undulator beamline 7.0 of the Advanced Light Source (ALS), Lawrence Berkeley National Laboratory with a spherical grating monochromator.⁴⁸ Ti 2*p* (L_{2,3}) XES and O 1*s* (K_α) XES spectra of these samples were recorded by using a Nordgren-type grating spectrometer.⁴⁹ The spectrometer was mounted perpendicular to the incoming photon beam in the polarization plane and the resolution was 0.3 eV and 0.4 eV, respectively, for Ti 2*p* and O 1*s* XES spectra. The monochromator was set to the excitation energies of 475 eV and 565 eV respectively, for Ti 2*p* and O K_α spectra with a resolution of 0.5 eV. The samples were mounted to have a beam incidence angle of 30° to sample surface. For energy calibration of the Ti 2*p* XES and O K_α XES, the spectra of the reference samples Ti, TiO₂, and Zn were measured. The base pressure of the chamber was 2 x 10⁻⁹ torr. The absorption spectra at the Ti 2*p* and O 1*s* edges were measured by means of total electron yield (TEY) and with a monochromator resolution set to 0.2 eV. The absorption intensity was normalized by the current from a clean gold mesh placed in the incoming beam to compensate for fluctuations of the incoming photon intensity. The XES and XAS spectra were brought to a common energy scale using an elastic peak in the emission spectra recorded at the excitation energy set at the absorption edge. The measurement depth of XAS is normally around 10 nm, and is around 100 nm for XES.

For XPS measurements, a Perkin-Elmer PHI 5600 XPS System was used. The energy resolution of the spectrometer was 0.3 - 0.5 eV. Samples for XPS measurement were coated on carbon tape attached to the sample holder. The charge compensation was applied to each sample to the characteristic peak at 284.6 eV of the carbon tape. The pressure in the vacuum chamber during the measurements was below 3 x 10⁻¹⁰ torr. The

XPS data were taken with a monochromated X-ray source (Al K_{α}). Ar^+ was applied to sputter the surface of the samples.

3. Results

3.1 Structural, Chemical and Optical Properties of N-, C- and S-doped TiO_2 as Compared to Pure TiO_2 .

TiN and TiC have NaCl-like cubic structure, with N or C atoms occupying interstitial positions in a close packed arrangement of Ti atoms.²¹ TiS_2 has a CdI_2 -like layered structure consisting of S-Ti-S slabs,^{24,39,50} with the Ti ions in a regular octahedral coordination to the sulfur ions.³⁹ The XRD in Fig. 1A shows that after heating treatment TiN, TiC and TiS_2 changed into TiO_2 -rutile phase. We designate the resultant samples after heating TiN, TiC and TiS_2 as $\text{TiO}_{2-x}\text{N}_x$, $\text{TiO}_{2-y}\text{C}_y$ and $\text{TiO}_{2-z}\text{S}_z$, which will be discussed later.

Fig. 1B shows the wide energy range XPS spectra of $\text{TiO}_{2-x}\text{N}_x$, $\text{TiO}_{2-y}\text{C}_y$ and $\text{TiO}_{2-z}\text{S}_z$ before Ar^+ sputtering. The XPS binding energies from the samples were calibrated with respect to the C 1s peak from the carbon tape at 284.6 eV. For all doped TiO_2 samples, typical binding energies for Ti 2p and O 1s were detected at 458.6 eV (for Ti $2p_{3/2}$) and 464.4 eV (for Ti $2p_{1/2}$), 530.5 eV, respectively. No apparent N, or S signals were detected on the surface. The strong C peak from all the samples appeared at 284.6 eV, so they were attributed to the carbon tape where the samples were put on. The top layers of these materials were completely transformed into pure TiO_2 . This phenomenon has been reported for TiN, TiC and TiS_2 when exposed to air even at room temperatures.¹⁶⁻

Shown in Figure 2 are the XPS spectra after the samples were sputtered for 1 min with the sputtering rate of 57 ± 20 Å/min. Ar^+ with 4 keV was used as sputtering source. The sputtering rate was estimated from the calibration with Ta_2O_5 material. In Fig. 2A, the peaks at 400.0 eV and 396.7 eV in the $\text{TiO}_{2-x}\text{N}_x$ were attributed to N $1s$ electrons within different Ti-N bonding environments.^{6-9,51-54} In Fig. 2B, the peak at binding energy 284.6 eV was due to C1s electrons from the carbon tape, and the peak at 281.8 eV was from to the Ti-C bond in the $\text{TiO}_{2-y}\text{C}_y$.^{14,25} In Fig. 2C of the $\text{TiO}_{2-z}\text{S}_z$, the peaks at 161.7 eV and 168.6 eV were attributed to the S $2p$ electrons in the S-Ti bond and the formed SO_2 species trapped in the lattice.^{26,55} The peaks in the Ti $2p_{3/2}$ XPS spectra in Fig. 2D at binding energies of 458.6⁵¹, 454.9,⁵⁶ 455.3⁵¹ and 456.4 eV⁵⁷ verified the O-Ti, N-Ti, C-Ti, and S-Ti bonds in the $\text{TiO}_{2-x}\text{N}_x$, $\text{TiO}_{2-y}\text{C}_y$ and $\text{TiO}_{2-z}\text{S}_z$ samples, respectively. The surface N, C and S dopant concentration was about 0.2%, 0.5% and 4.2% in atomic ratios, respectively, calculated by the ratio of the Ti, O, N, C, and S peaks after curve fittings and adjusted with their corresponding sensitivity factors. However, as the reviewers pointed out, the possibility of surface segregation covered by a layer of ambient adsorbates can not be fully ruled out.

Figure 3 shows the optical absorption spectra of TiN, TiC, TiS_2 and the $\text{TiO}_{2-x}\text{N}_x$, $\text{TiO}_{2-y}\text{C}_y$ and $\text{TiO}_{2-z}\text{S}_z$. TiN, TiC and TiS_2 have gray, black and black-gray color, and they display absorption from IR into UV regime (curves a, c, e). After heating, they changed into yellow color or slight yellow color (for TiS_2) (curves b, d, f). $\text{TiO}_{2-x}\text{N}_x$, $\text{TiO}_{2-y}\text{C}_y$ and $\text{TiO}_{2-z}\text{S}_z$ displayed bandgap absorption around 3.0 eV and long-tail absorption with peak positions around 2.76 eV (450 nm) and 2.0 eV (620 nm) as indicated by the arrows. The bandgap absorption was attributed to optical transitions of rutile TiO_2 host, and the long-

tail absorption was due to optical transitions involved with the electronic states modified by the N, C and S dopants in $\text{TiO}_{2-x}\text{N}_x$, $\text{TiO}_{2-y}\text{C}_y$ and $\text{TiO}_{2-z}\text{S}_z$.

3.2 XAS of $\text{TiO}_{2-x}\text{N}_x$ and Pure TiO_2

Fig. 4A shows XAS spectra from TiO_2 and $\text{TiO}_{2-x}\text{N}_x$ samples, obtained by the TEY method. For TiO_2 , below 469 eV, the Ti 2*p* XAS shows two bands, L_3 and L_2 , due to the 2*p* spin-orbit coupling.^{28,31,34} These further split into t_{2g} and e_g features because of the low symmetry of the TiO_6^{8-} ligand field O_h .^{28,31-34} Above 469 eV, there were weak and broad satellite peaks C, D and E, due to the Ti 2*p*, 4*s* and 4*p* states coupled with O 2*p* orbitals.³¹ The Ti 2*p* XAS of $\text{TiO}_{2-x}\text{N}_x$ is very similar to that of pure rutile TiO_2 . This suggests that the influence of the N dopant on the TiO_2 structure and crystal field is very small. One small difference was visible: the energy splitting for the center of Ti t_{2g} - e_g at the L_2 edge is larger in $\text{TiO}_{2-x}\text{N}_x$ (3.2 eV) than in TiO_2 (3.0 eV). This is attributed to possible crystal field changes due to the incorporation of the N atoms.

The O 1*s* XAS of the TiO_2 and $\text{TiO}_{2-x}\text{N}_x$ are shown in Fig. 4B. For TiO_2 , the low-energy range of the spectra (528-535 eV) was dominated by two strong broad bands, attributed to the oxygen 2*p* states hybridized with the empty split Ti 3*d* bands.^{27,28,31} The high-energy part of the spectrum was formed by the delocalized antibonding O 2*p* states coupled with Ti 4*sp* band with principally O 2*p* character.²⁸ The origin for the bands C-E was the same as analyzed above in the Ti XAS spectra. Peaks F and G were attributed to O 2*p* with some contribution from Ti 4*p*.^{27,31} The O 1*s* XAS of $\text{TiO}_{2-x}\text{N}_x$ was almost identical to that of TiO_2 . The identical spectra suggest that the N dopant does not affect

the O $2p$ orbitals in the $\text{TiO}_{2-x}\text{N}_x$ as compared to pure TiO_2 . This is reasonable, since the O is primarily bonded to the Ti, rather than the N atoms.

3.3 XES of $\text{TiO}_{2-x}\text{N}_x$ and Pure TiO_2

Figure 5 shows the XES spectra at the Ti $2p_{3/2}$ and O $1s$ edges in the TiO_2 and the $\text{TiO}_{2-x}\text{N}_x$ samples. The Ti $2p_{3/2}$ emission spectrum is due to the transition of electrons from Ti $3d$ states hybridized with O $2p$ states in the valence band into core holes on the Ti $2p_{3/2}$ level. The spectra from both $\text{TiO}_{2-x}\text{N}_x$ and pure TiO_2 (Fig. 5A) are very similar, with the exception that for $\text{TiO}_{2-x}\text{N}_x$, there is a small shoulder at the higher energy side (454.6 eV), likely due to Ti $3d$ states hybridized with N $2p$ states.^{29,32}

The O $1s$ (K-edge) x-ray emission spectra of both TiO_2 and the $\text{TiO}_{2-x}\text{N}_x$ (Fig. 5B) were almost identical, with one major peak at 525.0 eV and a smaller shoulder at 523.1 eV. The O K emission is due to the transition from the filled O $2p$ states to the O $1s$ hole state.²⁹ The same splitting energies between the main peak and the shoulder for TiO_2 and $\text{TiO}_{2-x}\text{N}_x$ is consistent with the idea that the change in the crystal field caused by N dopant is negligible, since the environment surrounding the O atoms is composed of Ti atoms at the same lattice sites in $\text{TiO}_{2-x}\text{N}_x$ as in pure TiO_2 .

3.4 Contribution of the N, C and S dopants to the electronic band structure of $\text{TiO}_{2-x}\text{N}_x$, $\text{TiO}_{2-y}\text{C}_y$ and $\text{TiO}_{2-z}\text{S}_z$

The XAS, XES and XPS spectra of pure rutile TiO_2 , $\text{TiO}_{2-x}\text{N}_x$, $\text{TiO}_{2-y}\text{C}_y$ and $\text{TiO}_{2-z}\text{S}_z$ are compared in Figure 6. The Ti $2p$, O $1s$ XAS and XES spectra for the N-, C- and S-doped TiO_2 were very similar or identical to those of pure TiO_2 as shown in Fig. 6A and

6B. This suggests that these N, C, and S dopants replacing the O atoms in the TiO₂ host do not significantly distort the Ti and O orbitals in the doped TiO₂ compared to pure TiO₂. In contrast to the XAS and XES, which probes the partial density of the conduction/valence band, the valence band XPS (VB XPS), probes a total density of the states distribution in the valence band.^{36,58-61} In the VB XPS spectra shown in Fig. 6C, there were additional widely dispersed electronic states above the valence band edge in TiO_{2-x}N_x, TiO_{2-y}C_y and TiO_{2-z}S_z compared to pure TiO₂. These states were apparently due to contributions of the N, C and S dopants in TiO_{2-x}N_x, TiO_{2-y}C_y and TiO_{2-z}S_z, respectively. This is consistent with previous reports by Asahi,⁸ Lindegren⁶² and Nakamura.⁶³

4. Discussion

4.1 The Structure, chemical composition and optical properties of N-, C- and S-doped TiO₂

The question arising here is whether the samples prepared are core/shell TiN/TiO₂, TiC/TiO₂ or TiS₂/TiO₂ structures, or N, C and S doped TiO₂. Core/shell TiN/TiO₂, TiC/TiO₂ or TiS₂/TiO₂ structures are easily excluded if we consider the different effective information depths in the XRD and XPS measurements. Usually in the XRD measurement, the effective information depth of X-ray can be larger than 10 μm from previous thin film studies.⁶⁴⁻⁶⁷ While in the XPS measurement, the effective information depth is normally around 5 nm.⁵⁸⁻⁶⁰ In the present study, there were no XRD signals from TiN, TiC nor TiS₂ for these samples, while, N, C and S were detected from the sputtering study, indicating that they lie within 10 nm of the surface. This suggests

that these samples are N, C and S-doped TiO₂ core with pure TiO₂ shell, with the dopants residing inside. The visible-light absorption was attributed to the N, C and S-doped TiO₂ core, since the penetration depth of light was larger than 10 μm and TiO₂ only absorbs UV-light. This is also confirmed from our lower temperature heating studies, where nanometer-sized anatase N, C and S-doped TiO₂ crystals can be obtained using the same method.⁶⁸

4.2 The electronic structure and bonding information provided from XAS, XES and XPS

Ti 2*p* XAS gives information regarding the unfilled band conduction band, while the 2*p* XES contains information about the filled portion of the 3*d*4*s* band (valence band).^{24,29} To a first approximation, the Ti 2*p* and O 1*s* XAS spectrum reflect the density of Ti 3*d* and O 2*p* unoccupied states (including hybrid states), the local coordination number and symmetry of a Ti and O ion in the material.^{28,32,33} The Ti 2*p* and O 1*s* XAS and XES spectra in these TiO_{2-x}N_x, TiO_{2-y}C_y and TiO_{2-z}S_z reflects the contribution of the TiO_{2-x} host. The similar Ti and O XAS and XES features for TiO_{2-x}N_x, TiO_{2-y}C_y, TiO_{2-z}S_z and pure TiO₂ suggested that N, C and S atoms substitutionally replaced the original O atoms in the rutile TiO₂ host, otherwise the different local coordination number and symmetry of a Ti atoms would induce different Ti 2*p* XAS and XES spectra in the doped TiO₂ host, i.e. the Ti e_g-t_{2g} splitting. The almost identical O 1*s* XAS and XES features for TiO_{2-x}N_x, TiO_{2-y}C_y, TiO_{2-z}S_z and pure TiO₂ suggested that N, C and S dopants had no influence on the O 2*p* orbitals. The tiny difference in the Ti XAS and Ti XES reflected the small effect of the N, C and S dopants on the Ti 3*d* orbitals in the doped materials.

Overall, the Ti and O XAS and XES suggested that the Ti and O orbitals in the doped and undoped TiO₂ were very similar.

The VB XPS spectra of TiO_{2-x}N_x, TiO_{2-y}C_y, TiO_{2-z}S_z and pure TiO₂ clearly displayed the contribution of the N, C, and S dopants to overall electronic structure of the doped TiO₂ in that these dopants induced additional electronic states brought above the edge of the TiO₂ valence states. This explained the visible-light absorption of TiO_{2-x}N_x, TiO_{2-y}C_y and TiO_{2-z}S_z. These experimental results were consistent with previous studies by Asahi,⁸ Lindegren⁶² and Nakamura.⁶³

5. Conclusions

Visible-light active N-, C- and S-doped TiO₂ were explored with XPS, XAS and XES in comparison with pure TiO₂. We found that the N, C and S dopants in the doped TiO₂ had only a small effect on the Ti 3d orbitals and the crystal structure of the original TiO₂. The VB XPS clearly displayed the modification of the electronic band structure of TiO₂ by the N, C and S dopants in these doped materials in that these dopants induced additional electronic states brought above the edge of the TiO₂ valence states. This explained the visible-light absorption of TiO_{2-x}N_x, TiO_{2-y}C_y and TiO_{2-z}S_z.

6. Acknowledgement

We thank C. McGuinness and F. de Groot for stimulating discussion. CB gratefully acknowledges financial support from NSF Grant (#CHE-0239688) and ACS-PRF. The work at Boston University is supported in part by the Department of Energy under DE-FG02-98ER45680. The Advanced Light Source is supported by the Director, Office of

Science, Office of Basic Energy Sciences, of the U.S. Department of Energy under
Contract No. DE-AC02-05CH11231.

7. References

- [1] M. R. Hoffmann, S. T. Martin, W. Choi and D. W. Bahnemann, Chem. Rev. 95(1995), 69.
- [2] M. Grätzel, Nature, 414(2001), 338.
- [3] A. Millis and S. L. Hunte, J. Photochem. Photobiol. A: Chem., 108(1997), 1.
- [4] A. L. Linsebigler, G. Lu and J. T. Yates Jr., Chem. Rev. 95(1995), 735.
- [5] A. Fujishima, T. N. Rao and D. A. Tryk, J. Photochem. Photobio. C: Photochem. Rev. 1(2000), 1.
- [6] X. Chen, Y. Lou, A. C. S. Samia, C. Burda and J. L. Gole, Adv. Funct. Mater. 15(2005), 41.
- [7] X. Chen and C. Burda. J. Phys. Chem. B 108(2004), 15446.
- [8] R. Asahi, T. Morikawa, T. Ohwak, K. Aoki and Y. Taga, Science 293(2001), 269.
- [9] C. Burda, Y. Lou, X. Chen, A. C. S. Samia, J. Stout and J. L. Gole, Nano Lett. 3(2003), 1049.
- [10] M. Miyauchi, A. Ikezawa, H. Tobimatsu, H. Irie and K. Hashimoto, Phys. Chem. Chem. Phys. 6(2004), 865.
- [11] S. Sakthivel and H. Kisch, Chem. Phys. Chem. 4(2003), 487.
- [12] T. Ohno, T. Mitsui and M. Matsumura, Chem. Lett. 32(2003), 364.
- [13] T. Umebayashi, T. Yamaki, S. Tanaka and K. Asai, Chem. Lett. 32(2003), 330.
- [14] H. Irie, Y. Watanabe and K. Hashimoto, Chem. Lett. 32(2003), 772.
- [15] D. W. Fischer and W. L. Baun, J. Appl. Phys. 39(1968), 4757.

- [16] F. Esaka, K. Furuya, H. Shimada, M. Imamura, N. Matsubayashi, H. Sato, A. Nishijima, A. Kawana, H. Ichimura and T. Kikuchi, *J. Voc. Sci. Technol. A* 15(1997), 2521.
- [17] L. Soriano, M. Abbate, J. C. Fuggle, P. Prieto, C. Jiménez, J. M. Sanz, L. Galán and S. Hofmann, *J. Voc. Sci. Technol. A* 11(1993), 47.
- [18] L. Soriano, M. Abbate, H. Pen, M. T. Czyżyk and J. C. Fuggle, *J. Electron Spectrosc. Relat. Phenom.* 62(1993), 197.
- [19] D. W. Fisher, *J. Appl. Phys.* 41(1970), 3922.
- [20] H. Ihara, Y. Kumashiro and A. Itoh, *Phys. Rev. B* 12(1975), 5465.
- [21] S. V. Didziulis, J. R. Lince, T. B. Stewart and E. A. Eklund, *Inorg. Chem.* 33(1994), 1979.
- [22] M. G. Faba, D. Gonbeau and G. Pfister-Guillouzo, *J. Electron Spectrosc. Relat. Phenom.* 73(1995), 65.
- [23] Z. Y. Wu, F. Lemoigno, P. Gressier, G. Ouvrard, P. Moreau and J. Rouxel, *Phys. Rev. B* 54(1996), R11009.
- [24] D. W. Fischer, *Phys. Rev. B* 8(1973), 3576.
- [25] Y. Choi, T. Umebayashi and M. Yoshikawa, *J. Mater. Sci.* 39(2004), 1837.
- [26] T. Umebayashi, T. Yamaki, H. Itoh and K. Asai, *Appl. Phys. Lett.* 81(2003), 454.
- [27] F. M. F. de Groot, J. Faber, J. J. M. Michiels, M. T. Czyżyk, M. Abbate and J. C. Fuggle, *Phys. Rev. B*, 48(1993), 2074.
- [28] Y. Hwu, Y. D. Yao, N. F. Cheng, C. Y. Tung and H. M. Lin, *NanoStruct. Mater.* 9(1997), 355.

- [29] D. W. Fischer and W. L. Baun, J. Appl. Phys. 39(1968), 4757.
- [30] A. Henningsson, H. Rensmo, A. Sandell, H. Siegbahn, S. Södergren, H. Lindström and A. Hagfeldt, J. Chem. Phys. 118(2003), 5607.
- [31] L. D. Finkelstein, E. I. Zabolotzky, M. A. Korotin, S. N. Shamin, S. M. Butorin, E. Z. Kurmaev and J. Nordgren, X-ray Spectrosc. 31(2002), 414.
- [32] Y. Harada, T. Kinugasa, R. Eguchi, M. Matsubara, A. Kotani, M. Watanabe, A. Yagishita and S. Shin, Phys. Rev. B 61(2000), 12854.
- [33] Y. Harada, M. Watanabe, R. Eguchi, Y. Ishiwata, M. Matsubara, A. Kotani, A. Yagishita and S. Shin, J. Electron Spectrosc. Related Phen. 114-116(2001), 969.
- [34] R. Ruus, A. Kikas, A. Saar, A. Ausmees, E. Nõmmiste, J. Aarik, A. Aidla, T. Uustare and I. Martinson, Solid State Comm. 104(1997), 199.
- [35] A. Augustsson, A. Henningsson, S. M. Butorin, H. Siegbahn, J. Nordgren and J. –H. Guo, J. Chem. Phys. 119(2003), 3983.
- [36] L. D. Finkelstein, E. Z. Kurmaev, M. A. Korotin, A. Moewes, B. Schneider, S. M. Butorin, J. –H. Guo, J. Nordgren, D. Hartmann, M. Neumann and D. L. Ederer, Phys. Rev. B 60(1999), 2212.
- [37] K. Okada and A. Kotani, J. Electron Spectros. Related Phenom. 62(1993), 131.
- [38] F. M. F. de Groot, J. Electron Spectros. Related Phenom. 62(1993), 111.
- [39] A. Šimůnek, O. Šipr, S. Bocharov, D. Heumann and G. Dräger, Phys. Rev. B 56(1997), 12232.

- [40] M. Georgson, G. Bray, Y. Claesson, J. Nordgren, C. –G. Ribbing and N. Wassdahl, J. Vac. Sci. Technol. A 9(1991), 638.
- [41] J. Nordgren, G. Bray, Y. Claesson, M. Georgson, C. G. Ribbing and N. Wassdahl, Surface Coat. Technol. 43-44(1990), 1275.
- [42] F. Esaka, K. Furuya, H. Shimada, M. Imamura, N. Matsubayashi, H. Sato, A. Nishijima, A. Kawana, H. Ichimura and T. Kikuchi, J. Vac. Sci. Technol. A 15(1997) 2521.
- [43] K. Dartigeas, L. Benoist, D. Gonbeau, G. Pfister-Guillouzo, G. Ouvrard and A. Levasseur, J. Electron Spectrosc. Relat. Phenom. 83(1997), 45.
- [44] S. V. Didziulis, J. R. Lince and T. B. Stewart, Inorg. Chem. 33(1994), 1979.
- [45] L. Porte, L. Roux and J. Hanus, Phys. Rev. B 28(1983), 3214.
- [46] M. J. Vasile, A. B. Emerson and F. A. Baiocchi, J. Vac. Sci. Technol. A 8(1990), 99.
- [47] J. L. Gole, J. D. Stout, C. Burda, Y. Lou and X. Chen, J. Phys. Chem. B 108(2004), 1230.
- [48] T. Warwick, P. Heimann, D. Mossessian W. McKinney and H. Padmore, Rev. Sci. Instrum. 67(1995), 2037.
- [49] J. Nordgren, G. Bray, S. Cramm, R. Nyholm, J. -E. Rubensson and N. Wassdahl, Rev. Sci. Instrum. 60(1989), 1690.
- [50] Y. Ohno, K. Hirama, S. Nakai, C. Sugiura and S. Okada, Phys. Rev. B 27(1983), 3811.
- [51] N. C. Saha and H. G. Tompkins, J. Appl. Phys. 72(1992), 3072.

- [52] O. Diwald, T. L. Thompson, E. G. Goralski, S. D. Walck and J. T. Yates, Jr. J. Phys. Chem. B 108(2004), 6004.
- [53] O. Diwald, T. L. Thompson, T. Zubkov, E. G. Goralski, S. D. Walck and J. T. Yates, Jr. J. Phys. Chem. B 108(2004), 52.
- [54] H. Irie, Y. Watanabe and K. Hashimoto, J. Phys. Chem. B 107(2003), 5483.
- [55] T. Umebayashi, T. Yamaki, S. Yamamoto, A. Miyashita, S. Tanaka, T. Sumita and K. Asai, J. Appl. Phys. 93(2003), 5156.
- [56] Y. Choi, T. Umebayashi, S. Yamamoto and S. Tanaka, J. Mater. Sci. Lett. 22(2003), 1209.
- [57] H. Martinez, C. Auriel, D. Gonbeau, M. Loudet and G. G. Pfister, Appl. Surf. Sci. 93(1996), 231.
- [58] S. Hufner, Photoelectron Spectroscopy: Principles and Applications, Springer-Verlag, New York, 1995.
- [59] M. Cardona, L. Ley, Photoemission in Solids I General Principles, Springer-Verlag, New York, 1978.
- [60] L. Ley, M. Cardona, Photoemission in Solids II: Case Studies, Springer-Verlag, New York, 1979.
- [61] M. Pedio, J. C. Fuggle, J. Somers, E. Umbach, J. Haase, T. Lindner, U. Hofer, M. Grioni, F. M. F. de Groot, B. Hillert, L. Becker and A. Robinson, Phys. Rev. B 40(1989), 7924.
- [62] T. Lindegren, J. M. Mwabora, J. J. Avendaño, A. Hoel, C. -G. Granqvist and S. -E. Lindquist, J. Phys. Chem. B 107(2003), 5709.
- [63] R. Nakamura, T. Tanaka and Y. Nakato, J. Phys. Chem. B 108(2004), 106717.

- [64] X. Chen, W. Yang, J. Liu and L. Lin, J. Membr. Sci. 255(2005), 201.
- [65] X. Chen, W. Yang, J. Liu and L. Lin. J. Mater. Sci. 39(2004), 671.
- [66] X. Chen, W. Yang, J. Liu, X. Xu, A. Huang and L. Lin J. Mater. Sci. Lett., 21(2002), 1023.
- [67] X. Xu, W. Yang, J. Liu, X. Chen, L. Lin, N. Stroh and H. Brunner, Chem. Commun. 7(2000), 603.
- [68] X. Chen. PhD Dissertation, Case Western Reserve University, Cleveland, OH, 2005.

Figure Caption:

Figure 1. (A) XRD patterns for the titanium compounds: (a) TiN; (b) $\text{TiO}_{2-x}\text{N}_x$; (c) TiC; (d) $\text{TiO}_{2-y}\text{C}_y$; (e) TiS_2 ; (f) $\text{TiO}_{2-z}\text{S}_z$, and (r) pure rutile TiO_2 . The $\text{TiO}_{2-x}\text{N}_x$, $\text{TiO}_{2-y}\text{C}_y$ and $\text{TiO}_{2-z}\text{S}_z$ display the typical diffraction pattern of rutile TiO_2 . (B) Before Ar sputtering, wide energy range XPS of $\text{TiO}_{2-x}\text{N}_x$, $\text{TiO}_{2-y}\text{C}_y$ and $\text{TiO}_{2-z}\text{S}_z$. The carbon 1s signals at 284.6 eV in the spectra were from the carbon tape.

Figure 2. After Ar^+ sputtering for 1 min, XPS spectra of the N-, C- and S-doped TiO_2 compared to that of pure rutile TiO_2 . (A) N 1s spectra for pure TiO_2 and $\text{TiO}_{2-x}\text{N}_x$, (B) C 1s spectra for pure TiO_2 and $\text{TiO}_{2-y}\text{C}_y$, (C) S 2p spectra for pure TiO_2 and $\text{TiO}_{2-z}\text{S}_z$; (D) Ti 2p spectra for pure TiO_2 and $\text{TiO}_{2-x}\text{N}_x$, $\text{TiO}_{2-y}\text{C}_y$ and $\text{TiO}_{2-z}\text{S}_z$.

Figure 3. Absorption spectra for the titanium compounds: (a) commercial TiN; (b) $\text{TiO}_{2-x}\text{N}_x$; (c) commercial TiC; (d) $\text{TiO}_{2-y}\text{C}_y$; (e) commercial TiS_2 ; (f) $\text{TiO}_{2-z}\text{S}_z$ and (r) pure rutile TiO_2 . The N-, C- and S-doped TiO_2 display the typical bandgap around 3.0 eV and additional lower energy tail absorption around 2.76 eV (450 nm) and 2.0 eV (620 nm) as indicated by the arrows.

Figure 4. XAS spectra of Ti 2p (A) and O 1s (B) in pure TiO_2 and $\text{TiO}_{2-x}\text{N}_x$ samples.

Figure 5. XES spectra of Ti L (A) and O K_α (B) in the TiO_2 and the $\text{TiO}_{2-x}\text{N}_x$ sample.

Figure 6. (A) Ti 2*p* XAS and Ti L XES spectra, (B) O 1*s* XAS and O K_α XES spectra and (C) XPS valence band spectra of pure rutile TiO₂, TiO_{2-x}N_x, TiO_{2-y}C_y and TiO_{2-z}S_z after sputtering for 1 min.

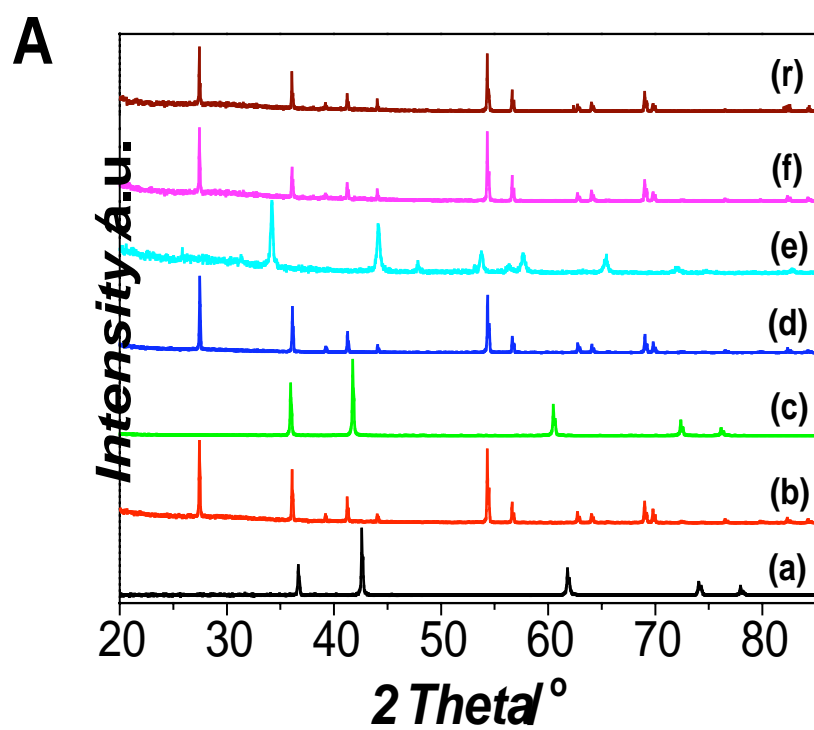


Figure 1A

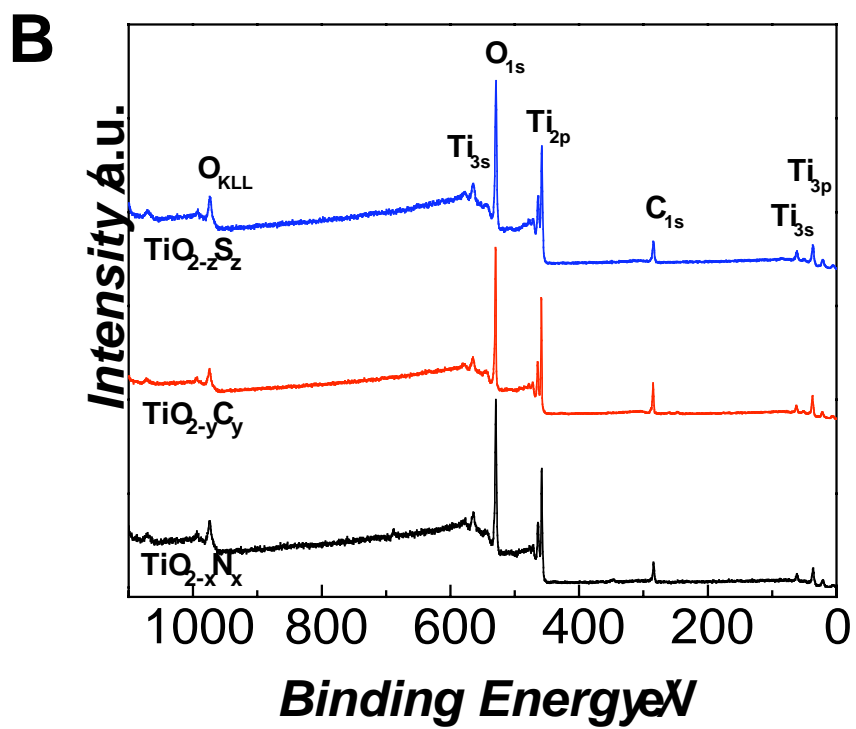


Figure 1B

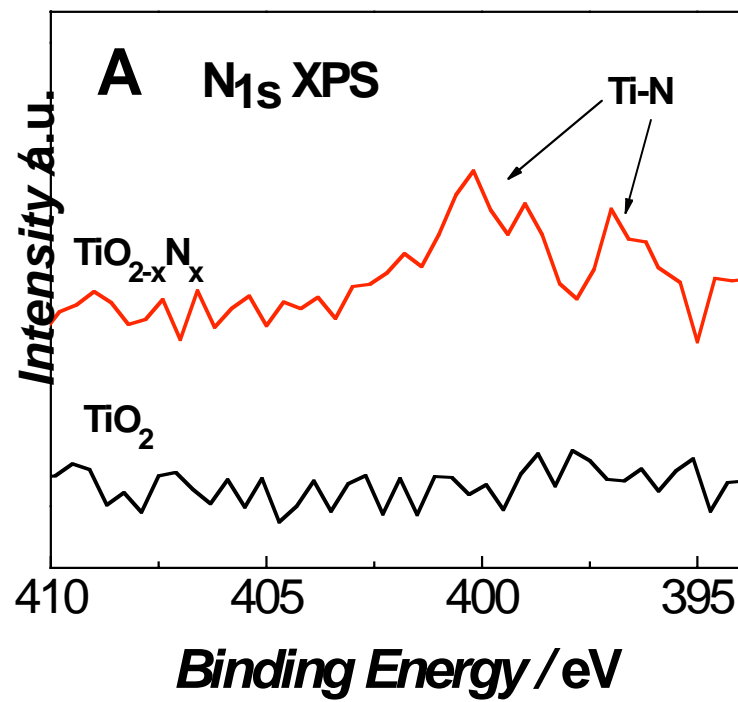


Figure 2A

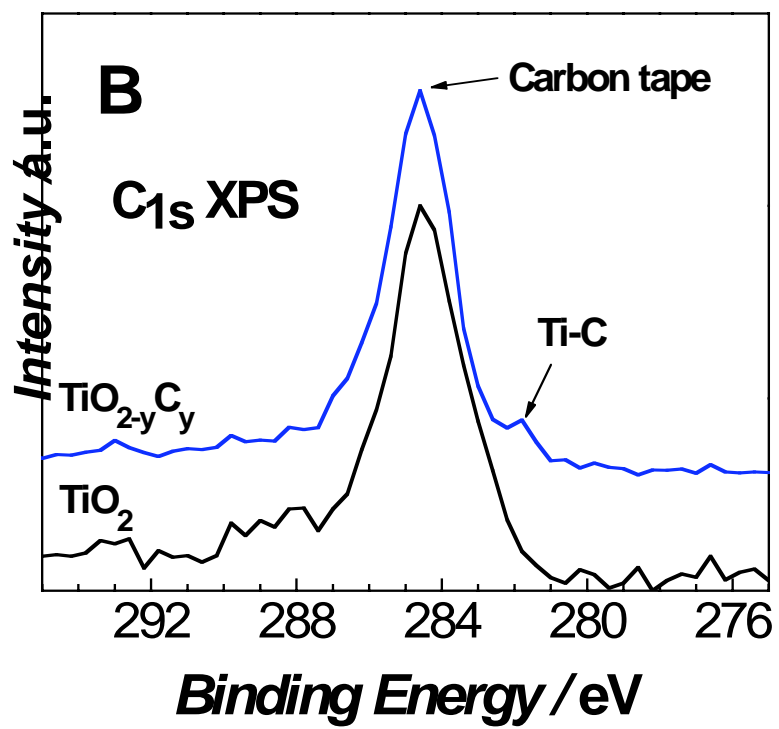


Figure 2B

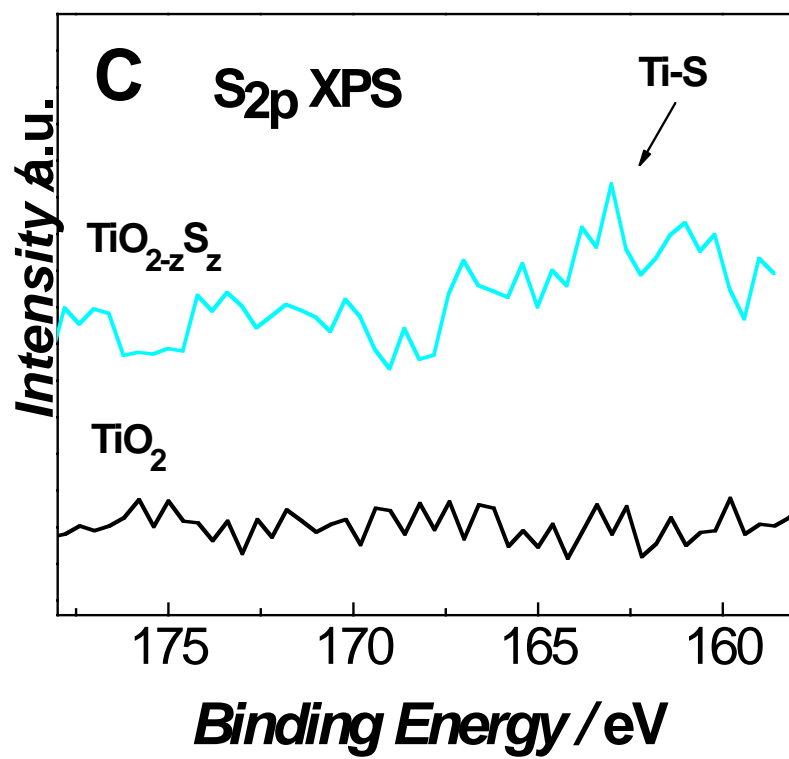


Figure 2C

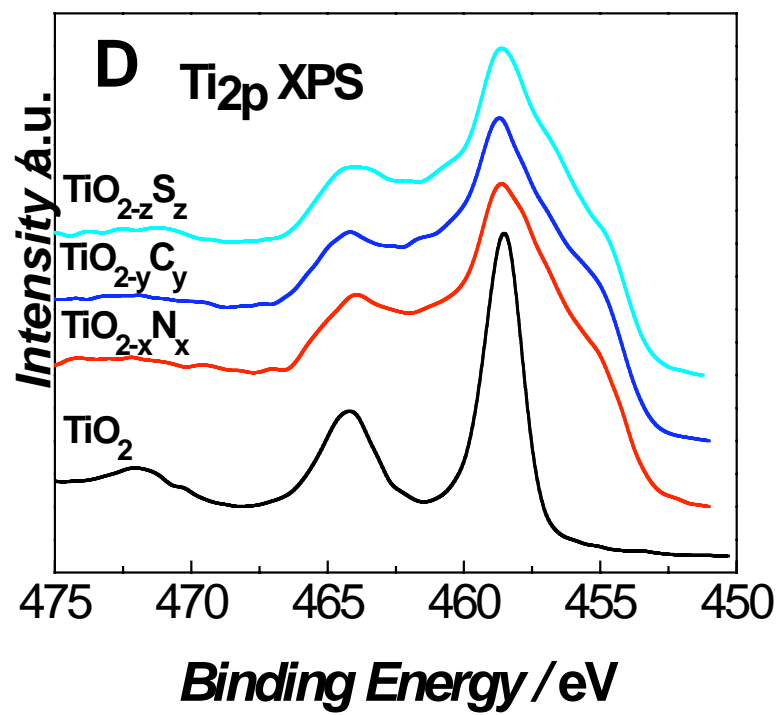


Figure 2D

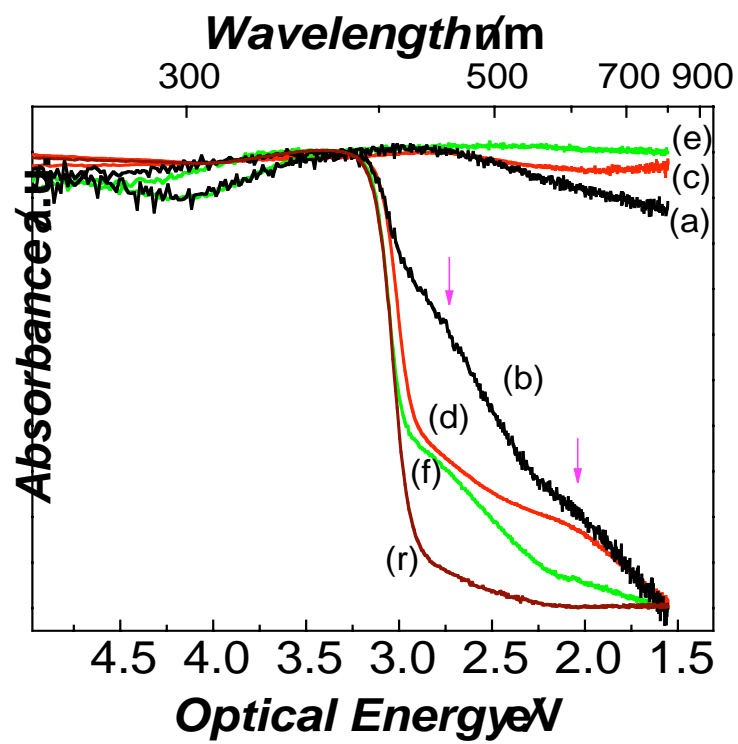


Figure 3

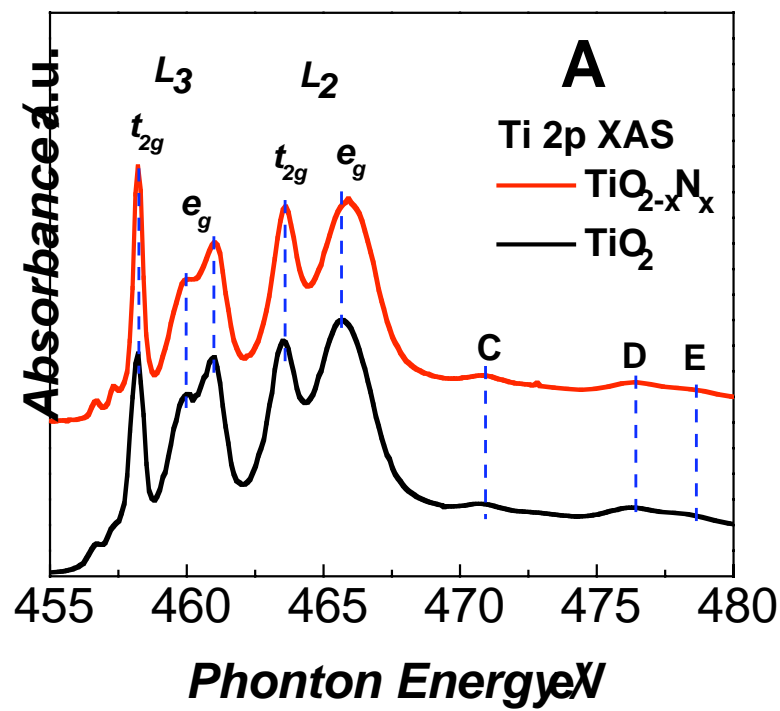


Figure 4A

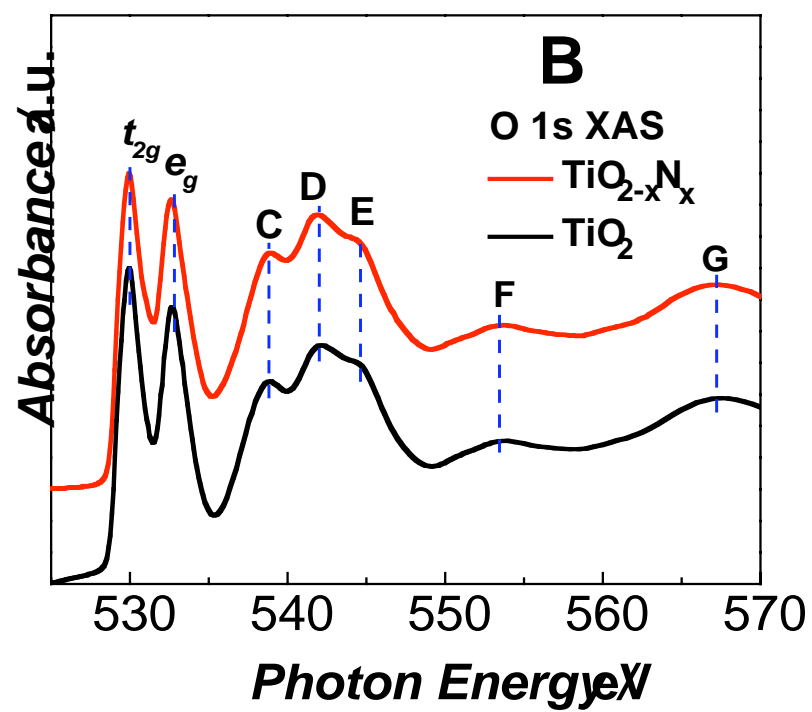


Figure 4B

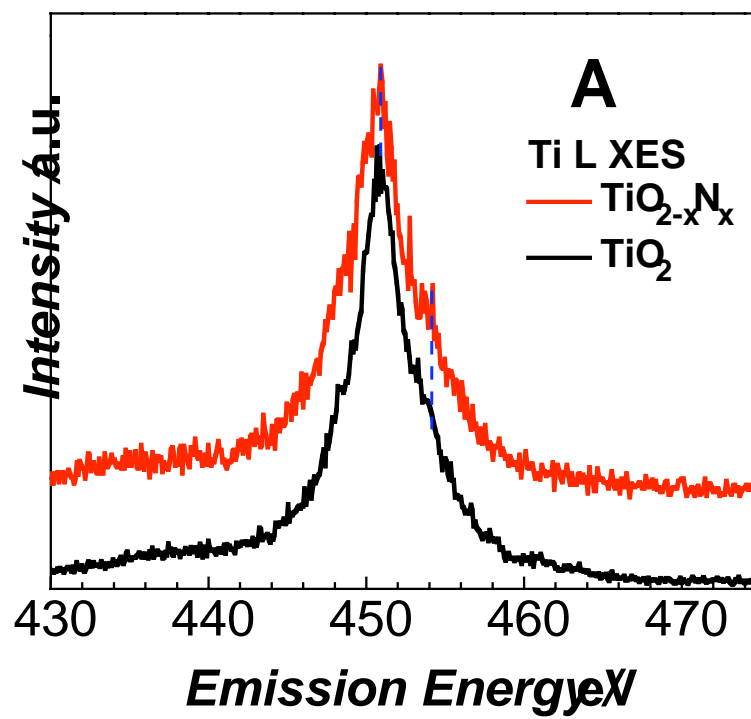


Figure 5A

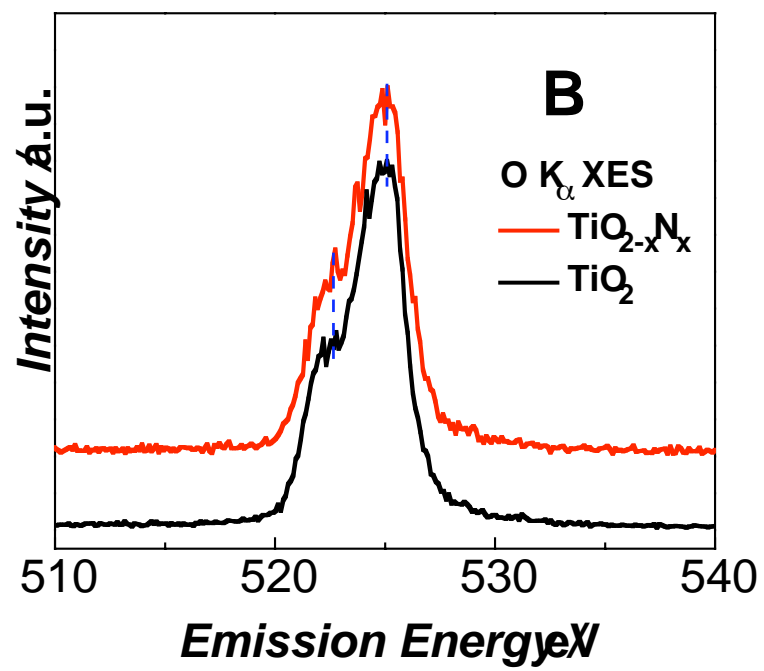


Figure 5B

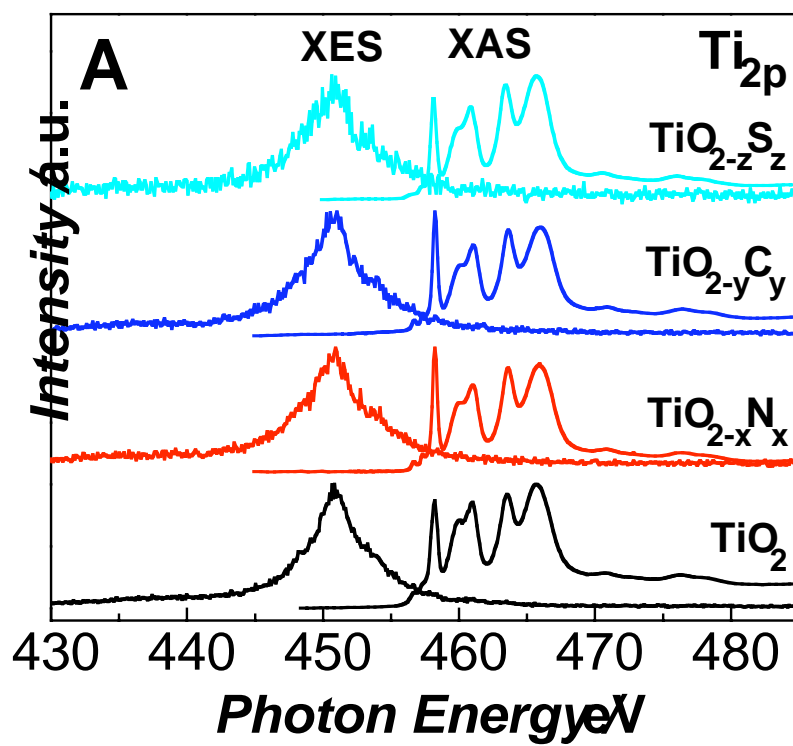


Figure 6A

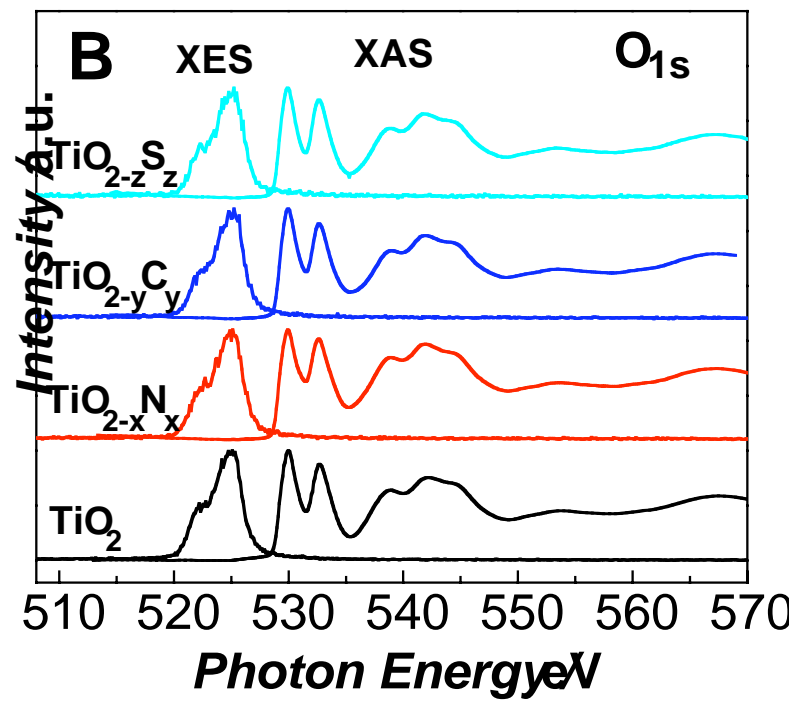


Figure 6B

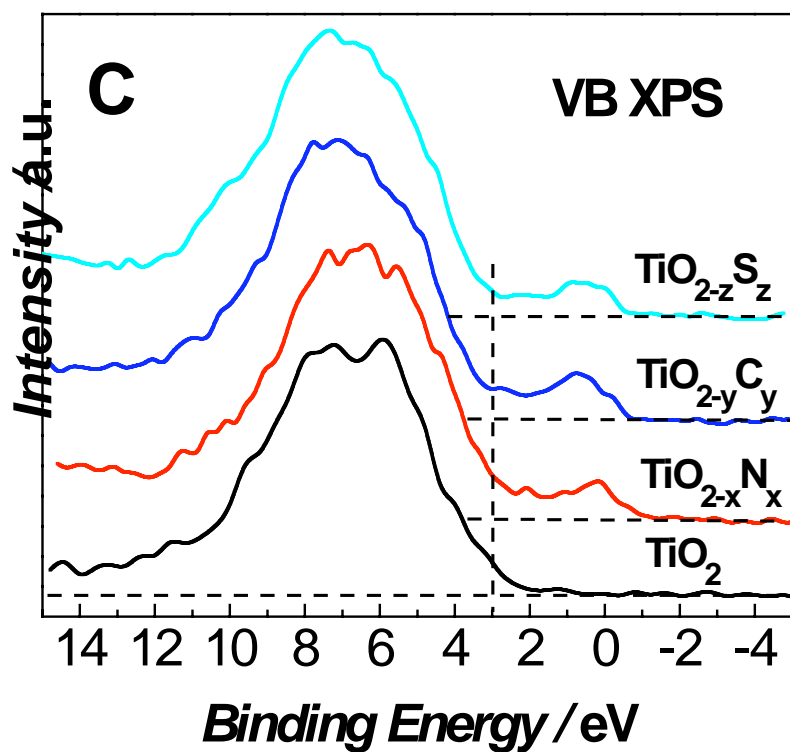


Figure 6C